



ELSEVIER

Available online at [www.sciencedirect.com](http://www.sciencedirect.com)

SCIENCE @ DIRECT®

Earth and Planetary Science Letters 233 (2005) 351–360

EPSL

[www.elsevier.com/locate/epsl](http://www.elsevier.com/locate/epsl)

## Rheology of fine-grained siliciclastic rocks in the middle crust—evidence from structural and numerical analysis

Ilse Kenis<sup>a,\*</sup>, Janos L. Urai<sup>b,1</sup>, Wouter van der Zee<sup>b,2</sup>,  
Christoph Hilgers<sup>b,3</sup>, Manuel Sintubin<sup>a,4</sup>

<sup>a</sup>*Structural Geology and Tectonics Group, K.U.Leuven, Redingenstraat 16, B-3000 Leuven, Belgium*

<sup>b</sup>*Geologie-Endogene Dynamik, RWTH Aachen, Lochnerstrasse 4-20, D-52056, Germany*

Received 22 September 2004; received in revised form 4 February 2005; accepted 5 February 2005

Available online 15 April 2005

Editor: R.D. van der Hilst

### Abstract

Constitutive models to describe the rheology of the crust are based on a combination of indirect methods, and many aspects are still unknown and controversial. Here we present a new method to quantify the rheology of fine-grained siliciclastic rocks, which are common in the middle crust and deform by solution-precipitation processes. We use a combination of structural analysis at different scales and a geomechanical model, to develop a parameter estimation scheme to calculate rheological parameters at 350–400 °C and geologic strain rates. The results of this study demonstrate that fine-grained siliciclastic rocks in the middle crust have a Newtonian viscous rheology, approximately 10 times weaker than wet quartz. This is in agreement with observed microstructures. Our results imply that the strength of polyphase quartz-rich rocks located in the middle crust is much lower than predicted by conventional models based on flow laws for dislocation creep. Because fine-grained siliciclastic rocks control the rheology of the middle crust in many sedimentary basins, our results provide new quantitative parameters for geodynamic modelling in settings where dissolution-precipitation creep is important.

© 2005 Elsevier B.V. All rights reserved.

*Keywords:* siliciclastic rocks; rheology; numerical model; mullions; middle crust

\* Corresponding author. Tel.: +32 16 326448; fax: +32 16 326401.

*E-mail addresses:* [ilse.kenis@geo.kuleuven.ac.be](mailto:ilse.kenis@geo.kuleuven.ac.be) (I. Kenis), [J.urai@ged.rwth-aachen.de](mailto:J.urai@ged.rwth-aachen.de) (J.L. Urai), [zee@geomi.com](mailto:zee@geomi.com) (W. van der Zee), [c.hilgers@ged.rwth-aachen.de](mailto:c.hilgers@ged.rwth-aachen.de) (C. Hilgers), [manuel.sintubin@geo.kuleuven.ac.be](mailto:manuel.sintubin@geo.kuleuven.ac.be) (M. Sintubin).

<sup>1</sup> Tel.: +49 2418095723; fax: +49 2418092358.

<sup>2</sup> Now at: GeoMechanics International, Emmerich Josefstrasse 5, 55116 Mainz, Germany.

<sup>3</sup> Tel.: +49 2418095723; fax: +49 2418092358.

<sup>4</sup> Tel.: +32 16 326447; fax: +32 16 326401.

### 1. Introduction

Geomechanical models form an essential basis for our quantitative understanding of tectonic processes. In these models, a long-standing problem involves the quantification of the constitutive equations that describe the rheology of the middle crust (7–12 km). Modellers commonly use generic viscosity contrasts

or laboratory-derived flow laws under the assumption that they can be extrapolated over several orders of magnitude to geological conditions (e.g. [1,2]). The brittle part of the crust is usually modelled using a frictional plastic rheology, whereas the ductile part is described using power-law creep equations based on dislocation creep of quartz or feldspar [3–11]. For the upper mantle, an olivine-controlled rheology is commonly assumed [12].

However, at present, laboratory methods are not sufficient to accurately constrain the rheology of rocks deforming in the subsurface at geologic strain rates [13]. Firstly a problem is that strength profiles are often based on rheological behaviour obtained from relatively low-strain experiments, which are 5 to 10 orders of magnitude faster than those found under normal geologic conditions. Secondly the rheology of rock mass in nature is controlled by polymineralic aggregates while laboratory experiments generally use monomineralic samples [14,15]. In addition to the polyphase character of natural rocks, factors contributing to the rheology of rocks include foliation development, and the action of fluid-assisted processes such as pressure solution [10]. For example, large portions of the crust in convergent margin settings deform by solution transfer creep in the presence of an aqueous phase instead of due to dislocation creep [16]. As a consequence the strength of polyphase quartz-rich rocks located in the middle crust may be much lower than predicted by conventional models based on flow laws from dislocation creep [7,10,16,17]. These aspects of crustal rheology have not been properly implemented in geodynamic models [1,2,16–18]. Additional constraints on rock rheology are needed from careful field- and observational studies and mechanical modelling.

Based on field data, attempts have been made to constrain viscosity contrast between different rocks in nature [19–26]. However, conversion of viscosity ratios derived from field data into a full set of rheological parameters has not yet been possible [27]. Therefore, the question ‘how soft is the crust’ is more alive than ever.

In this paper we present a combined structural and numerical analysis of fine-grained siliciclastic rocks deformed in the middle crust at around 350–400 °C. We use these as natural laboratories to quantify the

rheological parameters during flow at geologic strain rates.

The results of the analysis confirm the suggestion that polyphase quartz-rich rocks in the middle crust are significantly weaker than wet quartz and demonstrate that they behave in a linear or Newtonian way during deformation, as predicted by micromechanical models of solution-precipitation creep.

## 2. Mullions in layered siliciclastic rocks

The rock structures we analysed are mullions. Mullions are cusped–lobate folded layer interfaces, which form as a response to layer-parallel shortening. In the Ardenne–Eifel slate belt (Central Europe), mullions are common. The Ardenne–Eifel area is composed of low-grade metamorphosed siliciclastic multilayer sequences, which predominantly consist of pelites intercalated with fine-grained siliciclastic rocks rich in quartz, feldspar and phyllosilicates such as mica. In English literature, these fine-grained low-grade metamorphosed rocks are called psammites (e.g. [28–30]). In this paper we will use the term psammite according to this definition. The psammite layers of the High-Ardenne slate belt are characterized by the particular occurrence of arrays of lenticular quartz veins, which generally stop at the pelite–psammite interface (Figs. 1 and 2). In between the terminations of the quartz veins, the pelite–psammite interfaces show a cylindrical cusped–lobate fold geometry. These cusped lobate geometries represent the mullions. In general, the analysed structures have a two-stage history (Fig. 1). Firstly, the veins formed in regular arrays, by hydraulic fracturing during progressive burial, at near-lithostatic fluid pressure in the Rhenohercynian basin [31]. Secondly, subsequent layer-parallel shortening at the early stages of the Variscan orogeny resulted in folding of the pelite–psammite interface (i.e. formation of the mullions). This formation of mullions can be considered as the result of a rheological contrast between the vein quartz (q) and psammite (ps) [31,32]. The mullions were formed under low-grade metamorphic conditions (350–400 °C, 260 MPa, [33,34]), between about 335 and 325 Ma [35–37].

### 3. Microstructures

In the vein quartz, a number of microstructures characteristic for dislocation creep can be recognized. Large elongate-blocky quartz grains (500  $\mu\text{m}$  to 1 cm) show undulose extinction with the formation of subgrains. Dynamic recrystallization occurs by progressive rotation of subgrains and grain-boundary migration (Fig. 3a and b). The amount of undulose extinction and fraction of new grains are consistent with strains around 10%.

The microstructure of the pelite shows clear evidence of solution-precipitation creep, with a well-developed cleavage at high angle to the bedding.

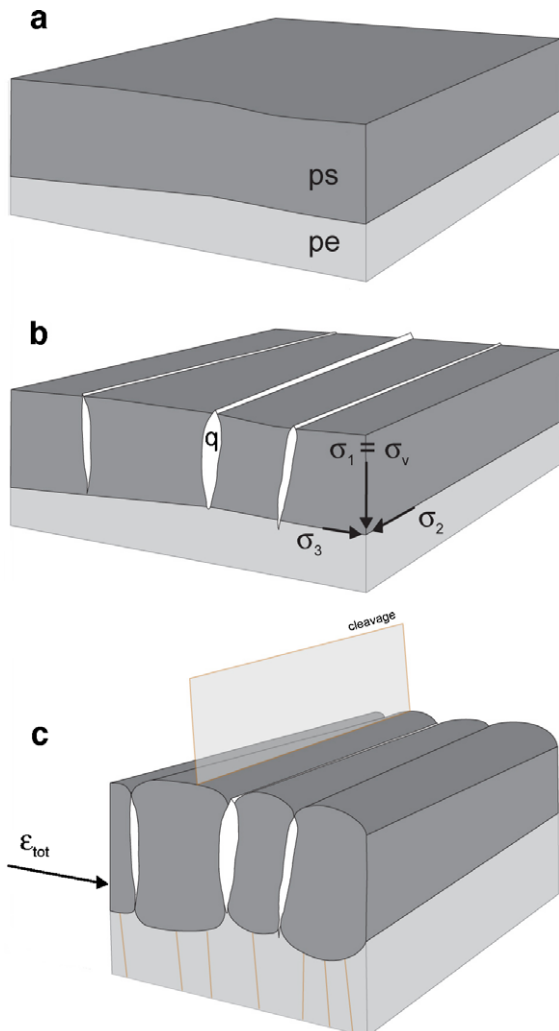


Fig. 1. Schematic illustration of the development of the analysed structures in the Ardenne–Eifel Slate Belt. (a) Layers of psammite (ps) and pelite (pe) are deposited and compacted during burial to depth of over 10 km in a passive continental margin. (b) Veins are formed in psammite layers after hydraulic fracturing in a high fluid pressure cell at the final phases of burial. (c) Layer-parallel shortening resulted in the formation of cusped–lobate geometries of the pelite–psammite interface (i.e. mullion formation) at the onset of Variscan compression. Vein quartz (q) is stronger than psammite (ps), which is in turn stronger than pelite (pe). The strength contrast between the vein quartz and psammite causes the formation of mullions in the layer interface of the psammite and pelite ( $\sigma_1$  is the maximum principal stress,  $\sigma_3$  the minimal principal stress,  $\sigma_2$  the intermediate principal stress;  $\sigma_v$  is the vertical total stress;  $\epsilon_{\text{tot}}$  is the total layer-parallel shortening).

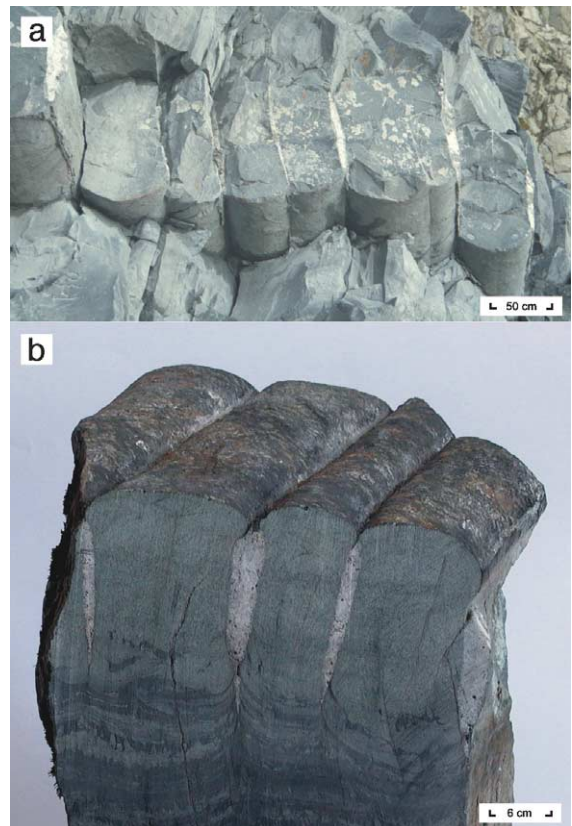


Fig. 2. Examples of mullions showing cylindrical cusped–lobate geometries of pelite–psammite interfaces, separated by quartz veins. In the third dimension, the veins are continuous and sub-parallel. (a) Mullions at Bastogne Mardasson ( $50^{\circ}1'50''\text{N}$ – $5^{\circ}44'20''\text{E}$ ) width of picture is 3 m; (b) mullions at Rouette ( $50^{\circ}03'10''\text{N}$ – $5^{\circ}39'30''\text{E}$ ), width of picture is 30 cm.

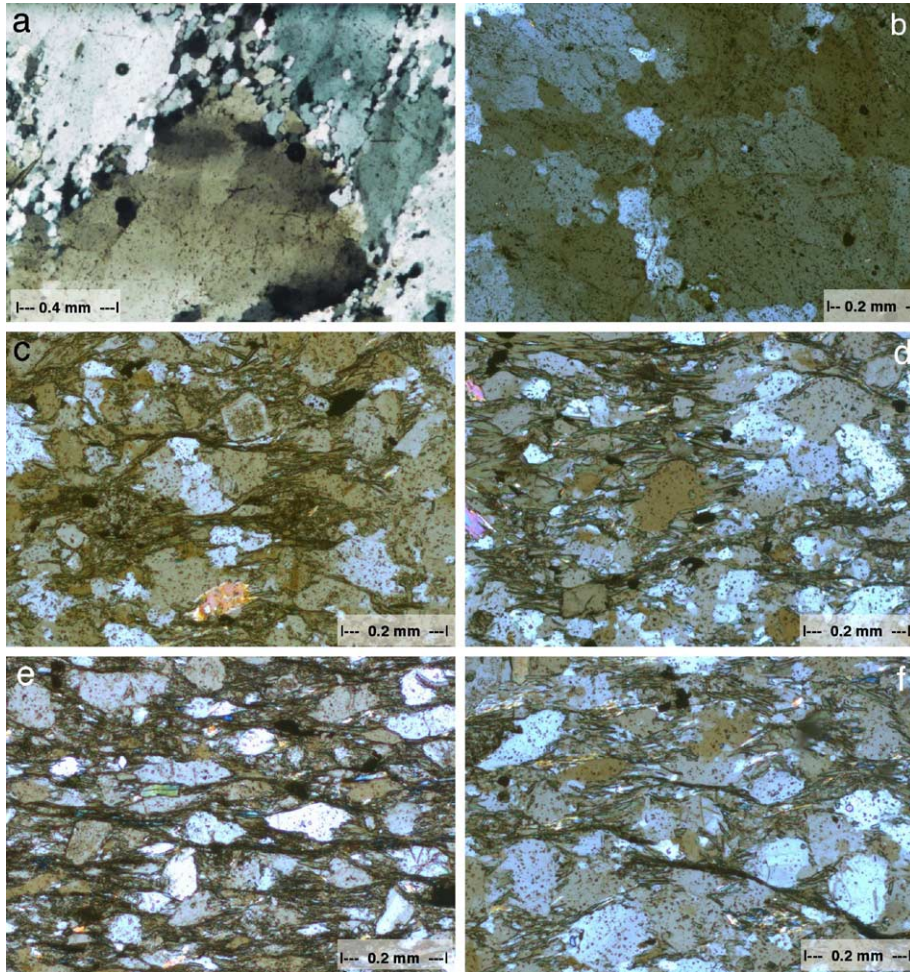


Fig. 3. (a–b) Microstructure of vein quartz characteristic for dislocation creep. Large elongate-blocky quartz grains (500  $\mu\text{m}$  to 1 cm) show undulose extinction with the formation of subgrains. Dynamic recrystallization occurs by progressive rotation of subgrains and grain-boundary migration. (c–f) Psammite matrix with microstructures characteristic for solution-precipitation creep. The original clastic shape of the grains can often be recognized, altered by preferential dissolution (e), overgrowth by quartz in strain fringes and in microboudin-necks (c,e). Grain aggregates are frequently overgrown by phyllosilicate beards (d) and phyllosilicate strain fringes are common.

In the psammite, although the much lower fraction of phyllosilicates prevents the development of a penetrative cleavage, there is also clear evidence for solution-precipitation creep (Fig. 3c–f). In quartz grains, undulose extinction is rare. The original clastic shape of the grains can often be recognized, altered by preferential dissolution (Fig. 3e), overgrowth by quartz in strain fringes and in microboudin-necks (Fig. 3c and e). Grain aggregates are frequently overgrown by phyllosilicate beards (Fig. 3d, cf. [38]) and phyllosilicate strain fringes are common also. In areas of

higher strain, close to the cusps and the vein tips, dissolution seams indicate localized areas of dissolution, and in the immediate vicinity of the cusps a well-developed cleavage is present, with truncated grains and microboudinage of elongated grains.

#### 4. Finite element mullion model

The simple, clearly defined geometry of most mullions provides an unusually well constrained set

of initial geometries and boundary conditions. This allowed the construction of a plane strain geomechanical model using finite element techniques [39,40]. For the three materials (pelite, psammite, vein quartz), we assume a volume-constant steady state power-law creep rheology ( $d\varepsilon/dt = A\Delta\sigma^n$ ) characterized by the corresponding parameters  $A_{pe}$ ,  $n_{pe}$ ,  $A_{ps}$ ,  $n_{ps}$ ,  $A_q$ , and  $n_q$ . Here,  $(d\varepsilon/dt)$  is strain rate ( $s^{-1}$ ),  $\Delta\sigma$  differential stress (MPa), and  $n$  the stress exponent. For vein quartz we use the relatively well-constrained wet quartz flow law of Hirth et al. [11], with  $A_q = A_0 f e^{(-Q/RT)}$  and  $n_q = 4$ . Here,  $A_0$  is material constant ( $10^{-11.2 \pm 0.6} \text{ MPa}^{-n}/s$ ),  $f$  water fugacity ( $\sim 38 \pm 2 \text{ MPa}$ ),  $Q$  activation energy ( $135000 \pm 15000 \text{ J/mol}$ ),  $R$  the gas constant and  $T$  the absolute temperature ( $623\text{--}673 \text{ K}$ ).

In a parameter sensitivity analysis [40], we have shown that the rheology of the pelite has almost no effect on the structures formed. Therefore, in agreement with results of earlier work [21,22,41], we assume a relationship between the rheology of psammite and pelite of  $A_{pe} = 5A_{ps}$ , and  $n_{pe} = n_{ps}$ . This assumption leaves psammite as the only material with unknown rheology.

The development of the shape of individual mullions is controlled by four parameters [40]: (1) total layer-parallel shortening, (2) initial aspect ratio of psammite segments before shortening, (3)  $n_{ps}$ , and (4) competence difference between vein quartz and psammite. The distribution of strain between vein quartz and psammite mainly depends on (4), while the curvature of the psammite–pelite interface is mainly a function of (3). (1) and (2) are parameters specific to individual mullions and can be obtained from strain analysis of mullions in the field.

The structural observations of a mullion in the field provide the opportunity to construct models specific to each mullion, using a suitably chosen set of parameters. Our sensitivity analysis suggests that there might exist a unique set of parameters, which makes the model match all the observations related to specific mullions. This would provide a tool to solve the inverse problem and determine the rheology of psammites.

### 5. Parameter estimation method

The method we used is a mixed numerical–structural parameter estimation scheme based on a

Table 1  
Case studies of mullions to determine the rheological properties of psammite ( $A_{ps}$  and  $n_{ps}$ )

Case	GP	$H-W$ (cm)	$\varepsilon_q$	$\varepsilon_{tot}$	$T$ (K)	AGS Q ( $\mu\text{m}$ )	$\Delta\sigma$ (MPa)	$A_{ps}$	$n_{ps}$	$t$ (s)
Boeur1	50°05'25"N–5°51'E	26–13	7.5 ± 2.5	22 ± 2.5	623 ± 10	53	41 ± 3	1.80*10 <sup>-15</sup> ± 1*10 <sup>-16</sup>	1 ± 0.2	2.52*10 <sup>13</sup> ± 8.8*10 <sup>12</sup>
Mardas3	50°01'50"N–5°44'20"E	80–43	7.5 ± 2.5	25.3 ± 2.1	658 ± 10	70	34 ± 3	6.1*10 <sup>-15</sup> ± 3*10 <sup>-16</sup>	1 ± 0.2	1.01*10 <sup>13</sup> ± 3.35*10 <sup>12</sup>
RouetteB	50°03'10"N–5°39'30"E	26–17	7.5 ± 2.5	31 ± 2	648 ± 10	74	32 ± 3	3.35*10 <sup>-15</sup> ± 1.15*10 <sup>-15</sup>	1 ± 0.2	2*10 <sup>13</sup> ± 6.65*10 <sup>12</sup>
RouetteC	50°03'10"N–5°39'30"E	26–10	5 ± 1	27 ± 1	648 ± 10	74	32 ± 3	4.3*10 <sup>-15</sup> ± 1*10 <sup>-16</sup>	1 ± 0.2	1.33*10 <sup>13</sup> ± 2.66*10 <sup>12</sup>
Sur les Roches	50°00'20"N–5°44'30"E	9–13	10 ± 1	27.8 ± 0.5	658 ± 10	88	29 ± 3	1.2*10 <sup>-15</sup> ± 1*10 <sup>-16</sup>	1 ± 0.2	2.54*10 <sup>13</sup> ± 1*10 <sup>12</sup>
Bertrix 1	49°52'40"N–5°13'30"E	25–8	10 ± 1	26.4 ± 0.5	663 ± 10	78	31 ± 3	8.2*10 <sup>-15</sup> ± 1*10 <sup>-16</sup>	1 ± 0.2	1.98*10 <sup>13</sup> ± 1*10 <sup>12</sup>
Bertrix 2	49°52'40"N–5°13'30"E	25–8	10 ± 1	26.4 ± 0.5	663 ± 10	78	31 ± 3	6.2*10 <sup>-15</sup> ± 1*10 <sup>-16</sup>	1 ± 0.2	1.98*10 <sup>13</sup> ± 1*10 <sup>12</sup>

GP is GPS coordinate of outcrop, ( $H-W$ ) is the initial height and width of the mullion,  $\varepsilon_q$  the finite strain of the vein quartz,  $\varepsilon_{tot}$  total strain,  $T$  temperature, AGS Q the average grain size of the recrystallized vein quartz,  $\Delta\sigma$  the differential stress calculated according to [26] and  $t$  duration of mullion formation. Solutions of the parameter estimation are  $A_{ps}$  and  $n_{ps}$ . It can be seen that  $n_{ps}$  of all case studies is very close to 1.

technique developed in material engineering [42–44]. Starting conditions are provided by reconstruction of the shape of the layers after vein formation, and an estimation algorithm is employed to determine the rheological parameters of the model. The solution corresponds to a set of parameters for which the difference between mullion constraints and numerical results is minimized. Below we first discuss the constraints provided by observations.

- (i) Optical microscopy indicates that the initially coarse-grained vein quartz was deformed and recrystallized (up to 30%) during mullion formation [31,32] (Fig. 3a–b). Based on the recrystallized fraction in the vein quartz, a finite strain of the veins between 5% and 10% is assumed [45]. Thus the vein quartz was clearly deformed, but less than the psammite. Differential stresses high enough to deform the quartz plastically were first present during the basin inversion. After formation of the mullions, when the regional folds developed a significant amplitude, most deformation was partitioned in the pelite during flexural flow, preventing further deformation of the mullions and quartz veins.
- (ii) The recrystallized grain size of vein quartz was used to estimate differential stress in the vein

during this deformation [46,47] (Table 1). Heterogeneities in microstructure did not allow measurement of the gradients in stress due to the lensoid shape of the vein (Fig. 4d), instead we measured an average value.

- (iii) The initial shape of the mullion was reconstructed assuming volume-constant deformation of the psammite and the above mentioned extension of the vein quartz. For the case studies reported below, the total layer-parallel shortening varies between 19% and 33% (Table 1).
- (iv) For our analyses, we selected mullions where the lithological interface between pelite and psammite layers can be confidently taken to be planar originally. These interfaces were digitized to allow comparison with the numerical solution.

The parameter estimation scheme and algorithm is as follows. For each individual mullion, we first determine the undeformed shape and construct a finite element mesh based on this. The total shortening imposed on the model is the ratio of their initial length and the observed length. Then, using the value of differential stress in the vein quartz, together with  $A_q$ ,  $n_q$ , and the total strain in the vein quartz (5–10%), we calculate the time required for deformation of the model. In all cases studied, this is well within time

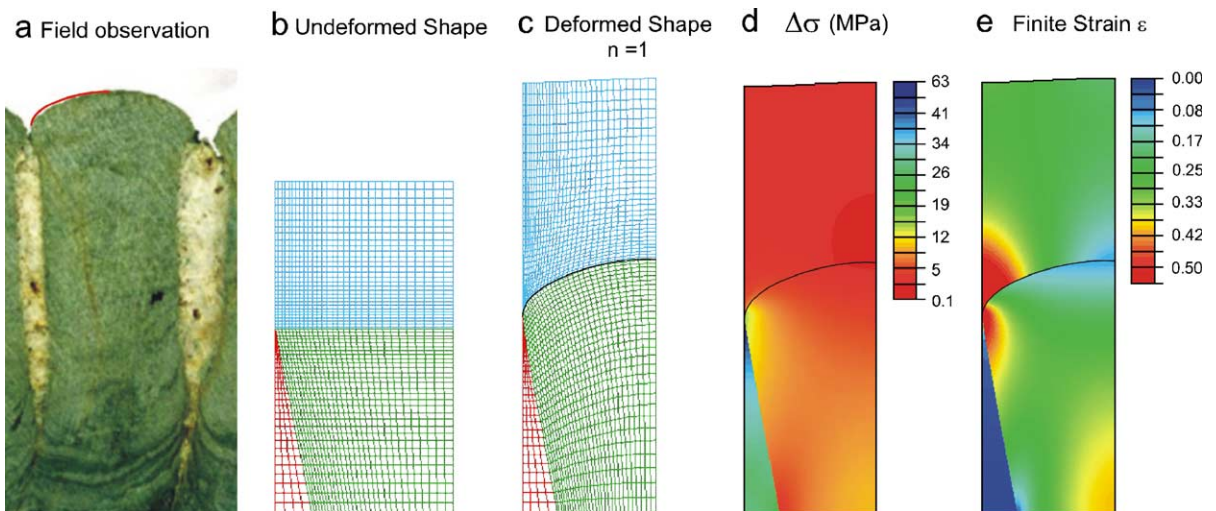


Fig. 4. Best fit solution of the case study of a mullion at Rouette ( $50^{\circ}03'10''\text{N}$ – $5^{\circ}39'30''$ ) showing field observation (a), undeformed (b) and deformed mesh (c) of the numerical model and contour plots of the differential stress (d) and finite strain (e) of the mullion structures. The result of the numeric solution fits well with observations of mullion shape. Stress and strain in the veins of the numerical solution are in agreement with constraints on these. Rheological properties ( $A_{ps}$ ,  $n_{ps}$ ) of this numeric solution are listed in Table 1 (Rouette C).

limits imposed by the geological constraints on duration of mullion formation. Next, based on the parameter sensitivity study [40], we make an initial estimate of  $A_{pe}$ ,  $n_{pe}$ ,  $A_{ps}$  and  $n_{ps}$ , with  $A_{pe}=5A_{ps}$ , and  $n_{pe}=n_{ps}$  and run a finite element calculation. Comparing the output of this model with the mullion constraints discussed above, we then adjust  $A_{pe}$ ,  $n_{pe}$ ,  $A_{ps}$  and  $n_{ps}$ , to lower the difference between model and observations and repeat the finite element calculation. We find that this rapidly leads to a model where the difference between model and mullion constraints reduces to values close to zero. The convergence is robust, because the effects of  $A$  and  $n$  are separate:  $n$  is mostly manifested in the curved shape of the pelite–psammite interface, and  $A$  affects the ratio in strain between psammite and vein quartz.

## 6. Rheology of psammite: case studies

To date, we have performed seven case studies (Table 1) of mullions observed in various outcrops. Using the parameter estimation method, in all cases the model converges to a single set of parameters, which define the flow law of fine-grained siliciclastic rocks, such as psammite, at low-grade metamorphic conditions and geologic strain rates. We consistently find an approximately 10-fold contrast in strength between the psammite and vein quartz, together with  $n_{ps}=1$  (Fig. 4). This indicates that psammite at low-grade metamorphic conditions deforms in a linear or Newtonian way. A Newtonian constitutive equation for the deformation behaviour of fine-grained siliciclastic rocks in the middle crust is in agreement with microstructural observations in the psammite, indicating that solution-precipitation creep was the dominant deformation mechanism active during ductile deformation [48]. Solution-precipitation creep was probably enhanced by the presence of phyllosilicates within the fine-grained siliciclastic rocks [17]. The absence of notable deformation by dislocation creep of quartz in the psammite indicates that the differential stress remained too low for this deformation mechanism to be competitive with dissolution-precipitation creep [48,49]. In contrast, the vein quartz is dominantly deformed by dislocation creep indicating higher flow stress in these parts and causing an inhomogeneous stress field in the different lithologies

(quartz vs. psammite), leading to the process of mullion formation during Variscan shortening.

Fine-grained siliciclastic rocks, such as the psammites described in this study, form large portions of the middle crust in siliciclastic sedimentary basins. The results in this study thus provide new quantitative data for geodynamic modelling demonstrating that fine-grained siliciclastic rocks in the middle crust are much weaker than supposed from conventional strength envelopes relying on flow laws for dislocation creep of wet quartz.

Mullions have been described in many settings, although they are not as common as folds or faults. Until now they were only of interest to specialized structural geology studies. In this study mullions are used as natural laboratories to quantify the rheological parameters during flow at geological strain rates. Using the parameter estimation scheme, we calculate the rheology of rocks in which the mullions are formed. This is possible due to the unusually well-constrained set of initial geometries and boundary conditions of the mullion formation. Our results apply to all psammites deformed under the same conditions, whether they contain mullions or not (mullions form because of the presence of bedding perpendicular quartz veins, and the absence of these does not alter the rheology). One does not need large numbers of mullions to determine the rheology in a particular setting.

## 7. Discussion

The assumptions made of our analysis are all reasonable. Firstly, steady-state creep is the dominant mode of deformation in the psammites, considering the strains involved. Therefore the inclusion of primary creep in the constitutive equation will not have a significant effect on the structures produced. Secondly, assuming no volume change in the deforming psammites and pelites is consistent with findings that state that during solution-precipitation creep volume flux caused by non-volatile element redistribution is mostly limited to the cm-scale [50]. In addition, this assumption is supported by the large variation in size (10 cm to 2 m) of mullions, which all have similar internal structures and can be modelled using similar rheological parameters. Because the

driving force of material transport during solution-precipitation creep is related to gradients in differential stress [51,52], one would expect differences between small and large mullions if volume flux is important.

Therefore, we conclude that the  $A_{ps}$  and  $n_{ps}$  values calculated using our parameter estimation scheme give a good description of the deformation of psammites at  $T=350\text{--}400\text{ }^{\circ}\text{C}$ , strain rate around  $10^{-15}\text{ s}^{-1}$ , in the presence of a water-rich fluid phase at pressures close to lithostatic.

We note that (as discussed above) the  $A_{ps}$  values depend on the flow law of quartz. A change in quartz flow law will result in a change of the  $A_{ps}$  in order to maintain a 10-fold contrast between psammite and quartz. On the other hand, the result of  $n_{ps}=1$  in all our case studies agrees with our observations of solution-precipitation creep and theoretical models of this process [49] and is independent of the vein quartz flow law used (Fig. 3c–f). We also note that the values of  $A_{pe}$  and  $n_{pe}$  are poorly constrained by this study, because the results of our models are insensitive to these parameters.

## 8. Conclusion

A Newtonian rheology for fine-grained siliciclastic rocks deforming in the middle crust has been suggested before, based on structural analysis or microstructural observations (e.g. [22]), but a convincing demonstration has been notoriously difficult. Using our numerical parameter estimation scheme in combination with structural analysis of mullions, we find that stress exponents of  $n=1$  and a flow strength approximately  $10\times$  less than wet quartz is the characteristic rheology of fine-grained siliciclastic rocks deforming in the middle crust at around  $350\text{--}400\text{ }^{\circ}\text{C}$ . The results of this study are in good agreement with the microstructures in the psammite showing that the dominant deformation mechanism in these fine-grained siliciclastic rocks during ductile deformation at  $350\text{--}400\text{ }^{\circ}\text{C}$  is pressure solution creep. As a consequence, the strength of polyphase quartz-rich rocks located in the middle crust is much lower than predicted by conventional models based on flow laws from dislocation creep. Because fine-grained siliciclastic rocks control the rheology of the

middle crust in many sedimentary basins, our results provide new quantitative parameters for geodynamic modelling in which a flow law for dissolution precipitation is essential. Moreover, mullions occur worldwide in deformed sediments, and the method is therefore applicable to quantify rock rheology in other areas and geological settings offering further perspective for the quantification of rheological flow laws.

## Acknowledgements

The manuscript benefited from the suggestions of D. Fisher and F. Simons. We thank E. Leroy, an anonymous reviewer and editor R. van der Hilst for their criticism and advice. Research of Janos Urai, Christoph Hilgers and Wouter van der Zee was funded by the Deutsche Forschungsgemeinschaft. Manuel Sintubin is a Research Associate of the Onderzoeksfonds-K.U.Leuven.

## References

- [1] C. Beaumont, J.A. Muñoz, J. Hamilton, P. Fullsack, Factors controlling the Alpine evolution of the central Pyrenees inferred from a comparison of observations and geodynamical models, *J. Geophys. Res.* 105 (2000) 8121–8145.
- [2] R. Cattin, J.P. Avouac, Modelling mountain building and the seismic cycle in the Himalaya of Nepal, *J. Geophys. Res.* 105 (2000) 13389–13407.
- [3] C. Goetze, B. Evans, Stress and temperature in the bending lithosphere, as constrained by experimental rock mechanics, *Geophys. J. R. Astron. Soc.* 59 (1979) 463–478.
- [4] M.S. Paterson, F.C. Luan, Quartzite rheology under geological conditions, in: R.J. Knipe, E.H. Rutter (Eds.), *Deformation Mechanisms, Rheology and Tectonics*, Geol. Soc. London, Spec. Publ., 1990, pp. 299–307.
- [5] G.C. Gleason, J. Tullis, A flow law for dislocation creep of quartz aggregates determined with the molten salt cell, *Tectonophysics* 247 (1995) 1–23.
- [6] R. Govers, M.J.R. Wortel, Extension of stable continental lithosphere and the initiation of lithosphere scale faults, *Tectonics* 14 (1995) 1041–1055.
- [7] D.L. Kohlstedt, B. Evans, S.J. Mackwell, Strength of the lithosphere: constraints imposed by laboratory experiments, *J. Geophys. Res.* 100 (1995) 17587–17602.
- [8] G. Ranalli, Rheology of the lithosphere in space and time, in: J.-P. Burg, M. Ford (Eds.), *Orogeny through Time*, Geol. Soc. London, Spec. Publ., vol. 121, 1997, pp. 19–37.
- [9] S. Karato, *Introduction to the Rheology and Dynamics of the Earth's Interior*, University of Tokyo Press, 2000.

- [10] B. Bos, C.J. Spiers, Frictional-viscous flow in phyllosilicate-bearing fault rock: microphysical model and implications for crustal strength profiles, *J. Geophys. Res.* 107 (2002), doi:10.1029/2001JB000301.
- [11] G. Hirth, C. Teysier, J. Dunlap, An evaluation of quartzite flow laws based on comparison between experimentally and naturally deformed rocks, *Int. J. Earth Sci.* 90 (2001) 77–87.
- [12] J. Jackson, Strength of the continental lithosphere: time to abandon the jelly sandwich? *GSA Today* (2002 September) 4–9.
- [13] E.B. Burov, The upper crust is softer than dry quartzite, *Tectonophysics* 361 (2003) 321–326.
- [14] S. Ji, R. Wirth, E. Rybacki, Z. Jiang, High-temperature plastic deformation of quartz–plagioclase multilayers by layer-normal compression, *J. Geophys. Res.* 105 (2000) 16651–16664.
- [15] M. Handy, S. Wissing, J.E. Streit, Strength and structure of mylonite with combined frictional-viscous rheology and varied bimineralic composition, *Tectonophysics* 303 (1999) 175–192.
- [16] S. Schwarz, B. Stöckhert, Pressure solution in siliciclastic HP-LT metamorphic rocks—constraints on the state of stress in deep levels of accretionary complexes, *Tectonophysics* 255 (1996) 203–209.
- [17] B. Stöckhert, M. Wachmann, M. Küster, S. Bimmermann, Low effective viscosity during high pressure metamorphism due to dissolution precipitation creep: the record of HP-LT metamorphic carbonates and siliciclastic rocks from Crete, *Tectonophysics* 303 (1999) 299–319.
- [18] J. Imber, R.E. Holdsworth, C.A. Butler, G.E. Lloyd, Fault-zone weakening processes along the reactivated Outer Hebrides Fault Zone, Scotland, *J. Geol. Soc. (Lond.)* 154 (1997) 105–109.
- [19] M.A. Biot, Theory of folding of stratified viscoelastic media and its implications in tectonics and orogenesis, *Geol. Soc. Amer. Bull.* 72 (1961) 1595–1631.
- [20] S.H. Treagus, A theory of finite strain variation through contrasting layers and its bearing on cleavage refraction, *J. Struct. Geol.* 5 (1983) 351–368.
- [21] S.H. Treagus, Are viscosity ratios of rocks measurable from cleavage refraction? *J. Struct. Geol.* 21 (1999) 895–901.
- [22] S.H. Treagus, J.E. Treagus, Studies of strain and rheology of conglomerates, *J. Struct. Geol.* 24 (2002) 1541–1567.
- [23] L. Lan, P.J. Hudleston, Finite element models of buckle folds in non-linear materials, *Tectonophysics* 199 (1991) 1–12.
- [24] L. Lan, P.J. Hudleston, Rock rheology and angular folds in single-layers, *J. Struct. Geol.* 18 (1996) 925–931.
- [25] P.J. Hudleston, L. Lan, Rheological controls on the shapes of single-layer folds, *J. Struct. Geol.* 16 (1994) 1007–1021.
- [26] N.S. Mancktelow, Finite-element modelling of single-layer folding in elasto-viscous materials: the effect of initial perturbation geometry, *J. Struct. Geol.* 21 (1999) 161–177.
- [27] C.J. Talbot, Can field data constrain rock viscosities? *J. Struct. Geol.* 21 (1999) 949–957.
- [28] R. Schmid, D. Fettes, B. Harte, E. Davis, J. Desmons, J. Siivola, Towards a unified nomenclature in metamorphic petrology: how to name a metamorphic rock, A proposal on behalf of the IUGS Sucommission on the Systematics of Metamorphic Rocks: provisional recommendations, web version of 14.01.2001, 2002.
- [29] R.L. Bates, J.A. Jackson, *Dictionary of Geological Terms*, Anchor Books, 1984.
- [30] A. Allaby, M. Allaby, *Dictionary of Earth Sciences*, Oxford University Press, 1999.
- [31] I. Kenis, M. Sintubin, P. Muchez, E.A.J. Burke, The “boudinage” question in the High-Ardenne slate belt (Belgium): a combined structural and fluid inclusions approach, in: P. Labaume, D. Craw, M. Lespinasse, P. Muchez (Eds.), *Tectonophysics*, vol. 348, 2002, pp. 93–110.
- [32] J.L. Urai, G. Spaeth, W. van der Zee, C. Hilgers, Evolution of mullion (formerly boudin) structures in the Variscan of the Ardennes and Eifel, *J. Virtual Expl.* 3 (2001) 1–15 (<http://www.virtualexplorer.com.au/2001/Volume3review/Urai2/index.html>).
- [33] A. Beugnies, Le métamorphisme de l’aire anticlinale de l’Ardenne, *Hercynica* 2 (1986) 17–33.
- [34] A. Darimont, E.A.J. Burke, J.L.R. Touret, Nitrogen-rich metamorphic fluids in devonian metasediments from Bastogne, Belgium, *Bull. Minéral.* 111 (1988) 321–330.
- [35] H. Ahrendt, N. Clauer, J. Hunziker, K. Weber, Migration of folding and metamorphism in the Rheinisches Schiefergebirge deduced from K–Ar and Rb–Sr age determinations, in: H. Martin, F.W. Eder (Eds.), *Intercontinental Fold Belts. Case Studies in the Variscan Belt of Europe and the Damara Belt in Namibia*, Springer, Berlin, 1983, pp. 323–338.
- [36] W. Fielitz, J.-L. Mansy, Pre- and synorogenic burial metamorphism in the Ardenne and neighbouring areas (Rhenohercynian zone, central European Variscides), in: M. Sintubin, S. Vandycke, T. Camelbeeck (Eds.), *Palaeozoic to Recent tectonics in the NW European Variscan Front Zone*, Volume, *Tectonophysics*, vol. 309, 1999, pp. 227–256.
- [37] O. Oncken, C. von Winterfeld, U. Dittmar, Accretion of a rifted passive margin: the Late Paleozoic Rhenohercynian fold and thrust belt (Middle European Variscides), *Tectonics* 18 (1999) 75–91.
- [38] S.F. Cox, M.A. Etheridge, Crack-seal fibre growth mechanisms and their significance in the development of oriented layer silicate microstructures, *Tectonophysics* 92 (1983) 147–170.
- [39] Hibbitt, Karlsson, and Sorensen, Inc., *ABAQUS/Standard User’s Manual (Version 6.2)*, 2002 Pawtucket, RI.
- [40] I. Kenis, J. Urai, W. van der Zee, M. Sintubin, Mullions in the high-ardenne slate belt (Belgium), numerical model and parameter sensitivity analysis, *J. Struct. Geol.* 26 (2004) 1677–1692.
- [41] S.H. Treagus, Modelling the bulk viscosity of two-phase mixtures in terms of clast shape, *J. Struct. Geol.* 24 (2002) 57–76.
- [42] M.A.N. Hendriks, Identification of the mechanical behaviour of solid materials [PhD thesis]: Eindhoven, University of Technology, The Netherlands, 1991.
- [43] M.A.N. Hendriks, C.W.J. Oomens, H.W.J. Jans, J.D. Janssens, J.J. Kok, A numerical experimental approach for the mechanical characterisation of composites, in: V. Askegaard (Ed.), *Proceedings of the 9th International Conference on Experimental Mechanics*, 1990, pp. 552–561.

- [44] M. Meuwissen, An inverse Method for the mechanical characterisation of metals [PhD thesis]: Eindhoven, University of Technology, The Netherlands, 1998.
- [45] J.L. Urai, W.D.M. Means, G.S. Lister, Dynamic recrystallization of minerals, *Am. Geophys. Union, Geophys. Monogr. (the Paterson volume)* 36 (1986) 161–199.
- [46] M. Stipp, S. Holger, R. Heilbronner, S.M. Schmid, Dynamic recrystallization of quartz: correlation between natural and experimental conditions, in: S. de Meer, M.R. Drury, J.H.P. de Bresser, G.M. Pennock (Eds.), *Deformation Mechanisms, Rheology and Tectonics: Current Status and Future Perspectives*, Geological Society, London, Special Publications, 200, 2002, pp. 171–190.
- [47] R.J. Twiss, Theory and applicability of a recrystallized grain size paleopiezometer, *Pure Appl. Geophys.* 155 (1977) 227–244.
- [48] E.H. Rutter, The kinetics of rock deformation by pressure solution, *Philos. Trans. R. Soc. Lond. Ser. A* 283 (1976) 203–219.
- [49] E.H. Rutter, Pressure solution in nature theory and experiment, *Geol. Soc. Lond.* 140 (1983) 725–740.
- [50] E.A. Erslev, D.J. Ward, Non-volatile element and volume flux in coalesced slaty cleavage, *J. Struct. Geol.* 16 (1994) 531–553.
- [51] D.W. Durney, Solution transfer, an important geological deformation mechanism, *Nature* 235 (1972) 315–317.
- [52] M.S. Paterson, Non-hydrostatic thermodynamics and its geological applications, *Rev. Geophys. Space Phys.* (1973) 355–389.